

Thermal-oxidative aging of DGEBA/EPN/LMPA epoxy system: Chemical structure and thermal–mechanical properties

Yan-min Pei^a, Kai Wang^{a,*}, Mao-sheng Zhan^a, Wen Xu^b, Xiao-jun Ding^b

^aKey Laboratory of Aerospace Materials and Performance (Ministry of Education), School of Materials Science and Engineering, Beihang University, No.37, Xueyuan Road, Beijing 100191, China

^bAerospace Research Institute of Materials and Processing Technology, Beijing 100076, China

ARTICLE INFO

Article history:

Received 3 February 2011

Received in revised form

8 April 2011

Accepted 25 April 2011

Available online 1 May 2011

Keywords:

Epoxy resin

Thermal-oxidative aging

DMTA

ATR-FTIR

ABSTRACT

The evolution of chemical structure and thermal–mechanical properties of diglycidyl ether of bisphenol-A and novolac epoxy resin blends cured with low molecular polyamide (DGEBA/EPN/LMPA system) during thermal-oxidative aging were investigated by Attenuated Total Reflectance Fourier Transform Infrared spectrometry (ATR-FTIR) and Dynamic Mechanical Thermal Analysis (DMTA). The results revealed that the chemical reactions during thermal-oxidative aging contained oxidation and chain scission. Some possible chemical reaction processes were given. There was a new compound formed during aging processes and the change of its glass transition temperature (T_g) with aging time followed an exponential law. In addition, the changes of dynamic mechanical behavior of this epoxy system aged at four different temperatures (110 °C, 130 °C, 150 °C, 170 °C) were compared. An empirical formula was obtained through kinetic analysis and this formula can be used to predict the oxidative degree of the surface at different aging temperature.

© 2011 Elsevier Ltd. All rights reserved.

1. Introduction

Materials derived from epoxy resin have been widely used in polymer industry such as adhesives, coatings, composites matrix, electrical insulating materials, and encapsulates for semi-conductors because of their remarkable properties for instance moderate mechanical properties, good chemical resistances, great electrical properties and excellent processability, etc [1–3]. However, during the service or storage of the epoxy resin the environment factors such as temperature, atmosphere, water, stress, etc can cause the deterioration of its properties, which greatly limits its application. In many cases, thermal degradation and oxidation are two important aging mechanisms. Therefore, it is necessary to study the thermal-oxidative aging mechanism of epoxy resin.

The thermal-oxidative aging of polymer involves physical and chemical aging. Physical aging [4] refers to structural relaxation of the glassy state toward the metastable equilibrium amorphous state, and it is accompanied by the increase of glass transition temperature and modulus of the epoxy system [5,6]. Chemical

aging mainly includes chemical structure changes of polymer resulting from high temperature, oxygen, water, etc. Many studies suggest that chemical reactions of epoxy resin during thermal-oxidative aging mainly contains post-cure [7–9], carbonyl growth [10–15], and chain scission [15–17], which leads to the darkening and decrease of its mechanic properties. There are many effective characterizing methods such as DSC [6,9,17–19], TG [13,19], DMTA [6,9,17,20], NMR [1,21], FTIR [10–14,22], XPS [11,23] and UV [10] for microstructure and properties evolution of epoxy resin during aging. FTIR and DMTA or DSC are proved to be the most effective measurements for isothermal-oxidative aging studies.

Diglycidyl ether of bisphenol-A epoxy resin (DGEBA) has a bad thermostability, and it is brittle for many applications. Some research [24–27] suggests that the thermostability and mechanical property of this resin system can be greatly improved by blended with a certain amount of novolac epoxy resin (EPN). However, the thermal-oxidative aging behavior of such a system has rarely been studied, and the influence of temperature on aging mechanism is not explicitly given in the present literatures of research on aging. In this article, low molecular polyamide (LMPA) 651 was selected as curing agent. Then the isothermal-oxidative aging behavior as well as the influence of temperature on thermal-oxidative aging mechanism of DGEBA/EPN/LMPA epoxy system was studied.

* Corresponding author. Tel./fax: +86 10 82338557.

E-mail address: wangkai@buaa.edu.cn (K. Wang).

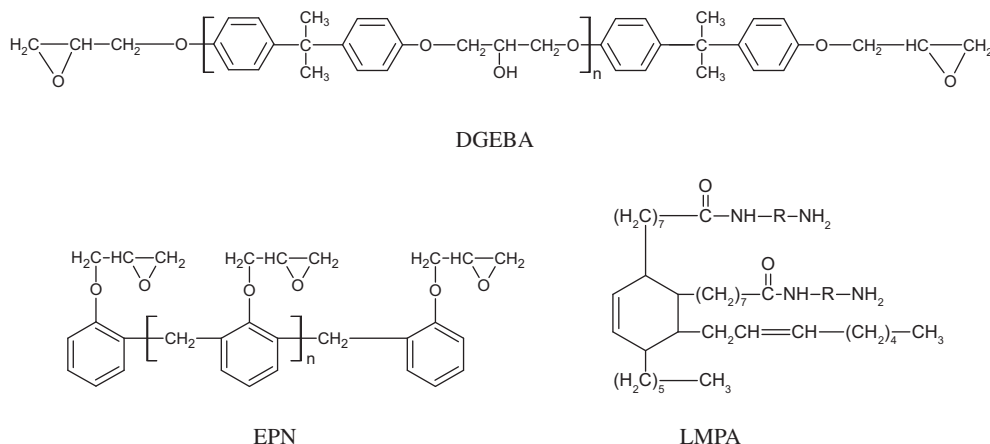


Fig. 1. Chemical structure of used materials.

2. Experimental

2.1. Materials and specimens preparation

The chemical structures of the compounds used in this study are detailed in Fig. 1. Diglycidyl ether of bisphenol-A (DGEBA) and novolac epoxy resin (EPN) were purchased from Wuxi Resin Factory, and low molecular polyamide (LMPA) 651 was supplied by Yan'an Chemical plant. The epoxy values of DGEBA and EPN are both 0.51 mol/100 g, R in the chemical structures of LMPA represent alkyl groups.

DGEBA/EPN/LMPA system was prepared first by blending DGEBA and EPN, and then being mixed with hardener (LMPA) with continuous stirring for 5 min. They were cured in the mold at 70 °C for 2 h after deaeration. DGEBA/LMPA and EPN/LMPA were prepared by mixing DGEBA and EPN respectively with an equivalent amount of hardener (LMPA).

2.2. Exposure conditions

Thermal-oxidative aging was carried out in ventilated ovens, ESPEC facilities (Japan) H201, set at four temperatures (110 °C,

130 °C, 150 °C and 170 °C), respectively. The specimens with 30.0 mm long, 8.0 mm wide and 2.0 mm thick were aged for the tests of DMTA, FTIR.

2.3. Techniques

2.3.1. Thermal–mechanical measurements

Thermal–mechanical tests were carried out using a Dynamic Mechanical Thermal Analyser (DMTA) from TA instrument company (USA) model 2980. The geometry of deformation was the three-point bending mode. The tests were performed in the scanning temperature mode, in the range from 0 to 300 °C, at a heating rate of 5 °C/min, and with an oscillating frequency of 1.0 Hz.

2.3.2. ATR-FTIR spectroscopy

The ATR-FTIR spectra were recorded with a Nexus 470 equipped with a Thunderdome-ATR (4 cm⁻¹ and 32 scans). The Thunderdome is a single reflexion ATR accessory with a germanium crystal.

The absorbance of absorption bands were obtained by formula (1),

$$A = \lg \frac{T_0}{T} \quad (1)$$

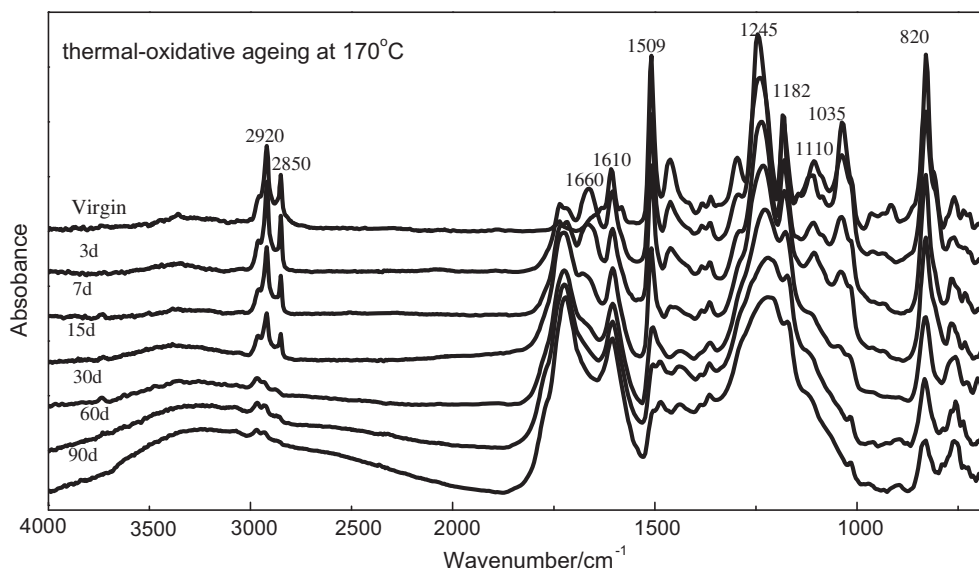


Fig. 2. IR spectra of DGEBA/EPN/LMPA epoxy system before and after aging at 170 °C for different time.

Table 1
Assignments of the characteristic absorption bands in ATR-FTIR spectra.

Absorption bands(cm^{-1})	Assignment
3330	Bending vibration of O–H
2920, 2850	Bending vibration of C–H– in methylene
1720	Stretching vibration of C=O– in saturated aldehyde, ketone or acid
1660	Stretching vibration of C=O in amide or diphenylketone
1610, 1509	Stretching vibration of C=C– skeleton in benzene ring
1245	Asymmetrical stretching vibration of C–O– ϕ
1182	Symmetrically stretching vibration of C–C
1110	Symmetrically stretching vibration of C–N
1035	Symmetrically stretching vibration of C–O– ϕ

where A is absorbance, T_0 is transmittance of baseline, and T is the transmittance of maximum absorption. The baseline was determined by the tangent method.

3. Results and discussion

3.1. ATR-FTIR analyses

The representative IR spectra of DGEBA/EPN/LMPA epoxy system obtained after aging at 170 °C for 0, 3, 7, 15, 30, 60, and 90 days are shown in Fig. 2. The assignments of the characteristic absorption bands of DGEBA/EPN/LMPA epoxy system in ATR-FTIR spectra are shown in Table 1.

After the exposure at hot air conditions, methylene in the network may be oxidized to carbonyl. The absorption band near 1660 cm^{-1} is the characteristic of stretching vibration of C=O in amide or diphenylketone. The observed increase in intensities of 1660 cm^{-1} band can be attributed to the formation and the growth of amide or diphenylketone. It is also evident from Fig. 2 that the characteristic absorption bands of near 2920 cm^{-1} and 2850 cm^{-1} decrease in intensity. These phenomena demonstrate that C–H

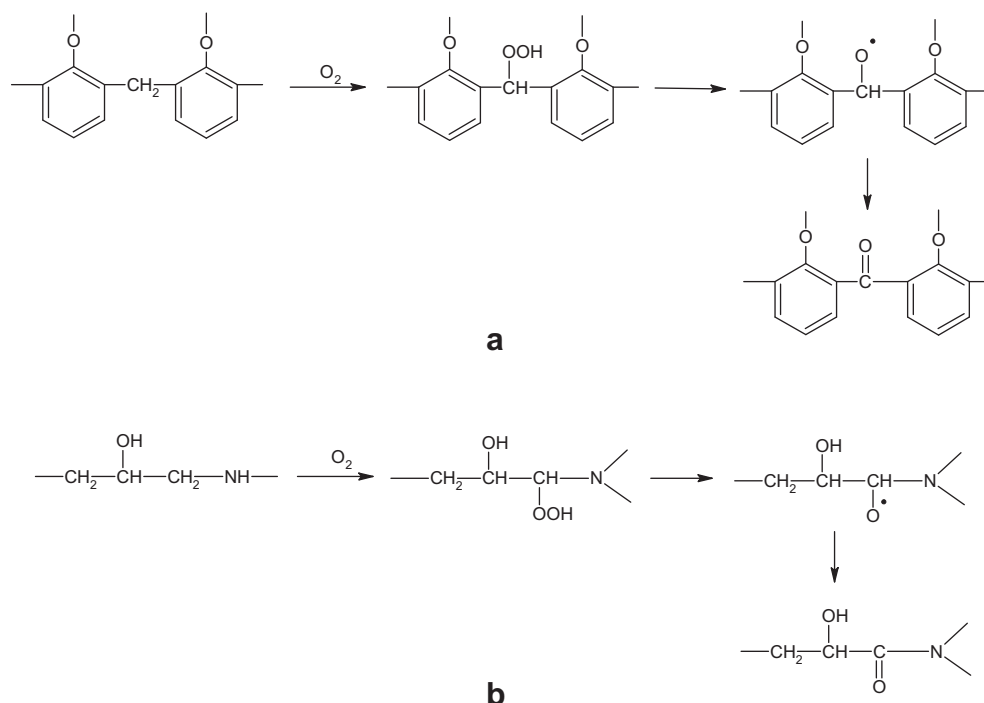
bond in methylene between two benzene rings or C–H bond in α of nitrogen atom in amine is oxidized, which results in the formation of amide [12,13] and diphenylketone [11] (as shown in Scheme 1a and b).

The samples of DGEBA/LMPA and EPN/LMPA were also aged at 170 °C, respectively. The absorption bands near 1660 cm^{-1} appeared in FTIR spectra of both systems. For DGEBA/LMPA system, it should be attributed to the formation of amide. For EPN/LMPA system, it should be attributed to the formation of not only amide but also diphenylketone groups because the intensity of the band near 1660 cm^{-1} is stronger for EPN/LMPA system at the same curing agent level and aging condition.

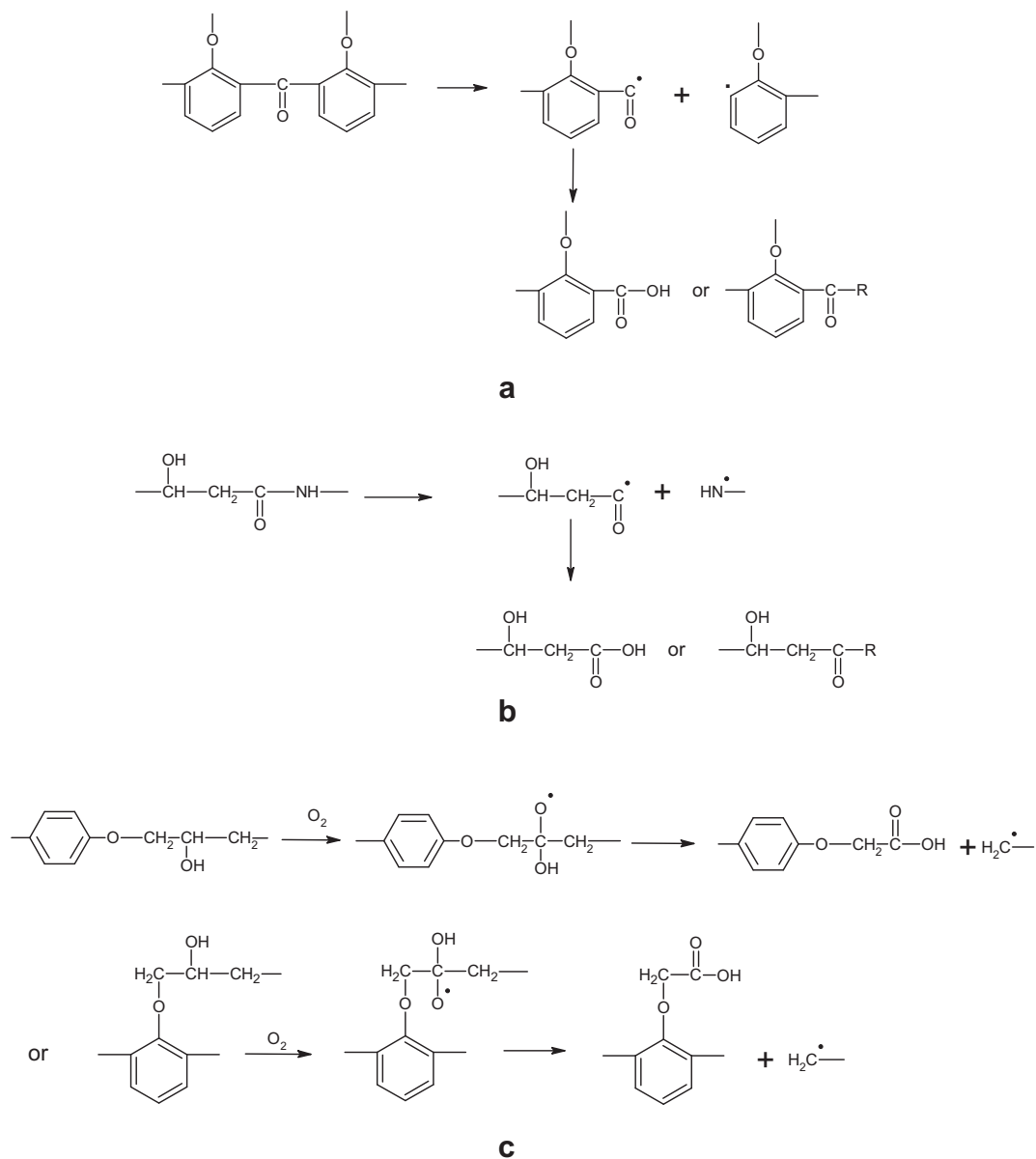
In addition, the characteristic absorption band of benzene ring near 1610 cm^{-1} increases in intensity with aging process, which attributes to the increasing polarity of substituent group. Meanwhile, the absorption band near 1509 cm^{-1} decreases in intensity, owing to the conjugate action between substituent group and benzene ring. Hence the formation of diphenylketone can be confirmed.

After aging for 15 days, the characteristic band of C=O in saturated aldehyde, ketone or acid near 1720 cm^{-1} appears and then increases with the decrease of the band near 1660 cm^{-1} , 1110 cm^{-1} (symmetrically stretching vibration of C–N) and 1182 cm^{-1} (symmetrically stretching vibration of C–C). This demonstrates that the bond of C–N in amide and C–C between carbonyl and benzene in diphenylketone has been destroyed and saturated aldehyde, ketone or acid has been formed (as shown in Scheme 2a and b).

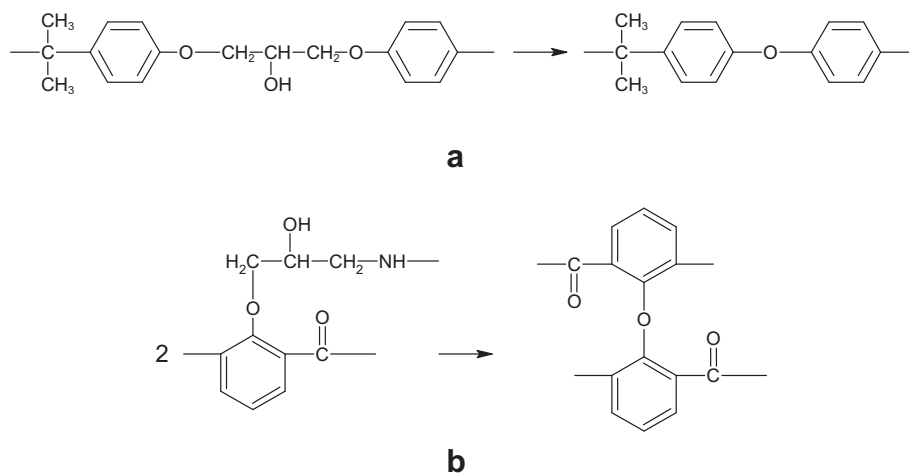
After a period of 30 days, the band near 1660 cm^{-1} , 1110 cm^{-1} and 1182 cm^{-1} disappear, which manifests that the structures of amide and diphenylketone have been destroyed completely. However, after 30 days the band near 1720 cm^{-1} continues increasing, which can be attributed to the formation of saturated aldehyde, ketone or acid at other positions. It has been reported by massive literatures [10–15], and the possible reactions are summarized as Scheme 2c.



Scheme 1. Possible reactions producing the amide and diphenylketone (absorption band near 1660 cm^{-1}).



Scheme 2. Possible reactions producing acids (absorption band near 1660 cm^{-1} decrease, near 1720 cm^{-1} appears and increase).



Scheme 3. Possible reactions producing $\phi\text{-O-}\phi$.

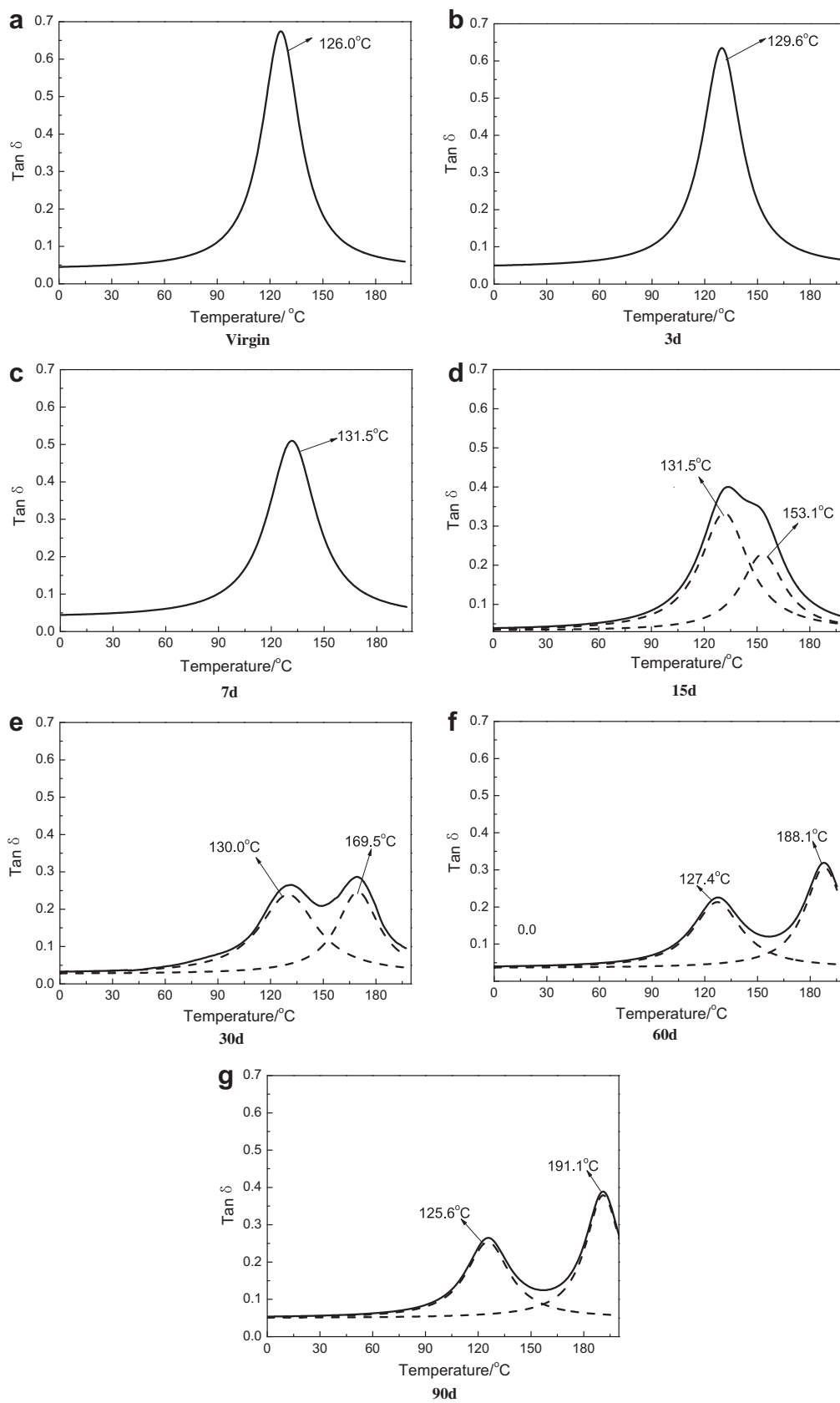


Fig. 3. The loss factors, $\tan \delta$, over temperature in different aging time (The solid curves represent the original data, and the dash lines are relative to the result after multi-peak resolution).

The absorption band near 1035 cm^{-1} , which derives from symmetrically stretching vibration of $\text{C}-\text{O}-\varphi$ [28,29] (φ represents benzene ring), decreases in intensity until it disappears. These results indicate that $\text{C}-\text{O}-\varphi$ is destroyed. Furthermore, the absorption band near 1245 cm^{-1} , deriving from asymmetrical stretching vibration of $\text{C}-\text{O}-\varphi$, moves toward lower wave number and is broadened, which can demonstrate the formation of $\varphi-\text{O}-\varphi$. The possible reaction is shown in Scheme 3.

In brief, aliphatic amines are oxidized to amide, methylene bridges in novolac epoxy are oxidized to ketone groups, and methylenes in other sites are also oxidized. In addition, $\text{C}-\text{C}$, $\text{C}-\text{N}$ and $\text{C}-\text{O}$ bonds break in the later stage of thermal-oxidative aging, and $\varphi-\text{O}-\varphi$ is formed.

3.2. DMTA analyses

The dynamic mechanical relaxation behaviors of DGEBA/EPN/LMPA system before and after aging at $150\text{ }^\circ\text{C}$ are studied. The loss factors, $\tan \delta$, measured as a function of temperature are shown in Fig. 3. The solid curves represent the original data, and the dotted lines the results after multi-peak resolution. The glass transition temperature, T_g , is defined by the $\tan \delta$ peak.

After 15 days' thermal-oxidative aging at $150\text{ }^\circ\text{C}$, it is observed that a secondary peak appears in $\tan \delta$ at higher temperatures. There are three possible explanations: DGEBA/EPN/LMPA settles into two separate phases of DGEBA/LMPA and EPN/LMPA; new compound with high concentration of crosslink density forms and appears in the system as a new phase; "skin-core" structure [30] forms for different degree of oxidation in the exterior and interior of the samples.

The DMTA measurement of the sample of DGEBA/LMPA system aged at $170\text{ }^\circ\text{C}$ show that a secondary peak appears in $\tan \delta$ at higher temperatures after 3 days, and this transition temperature increases with ongoing of aging time. Therefore, the appearance of the new transition peak in DGEBA/EPN/LMPA system is not caused by the separation of DGEBA/LMPA and EPN/LMPA.

After taking the brunet oxidation layer off the surface of the sample aged 90 days at $150\text{ }^\circ\text{C}$, the remainder was investigated by DMTA again. The result is shown in Fig. 4. For the treated sample, only one transition at $125\text{ }^\circ\text{C}$ is observed, which indicates that for the untreated sample the transition at $125\text{ }^\circ\text{C}$ and $191\text{ }^\circ\text{C}$ should be respectively attributed to the glass transition of the compound in the interior and exterior. The degrees of oxidation and degradation

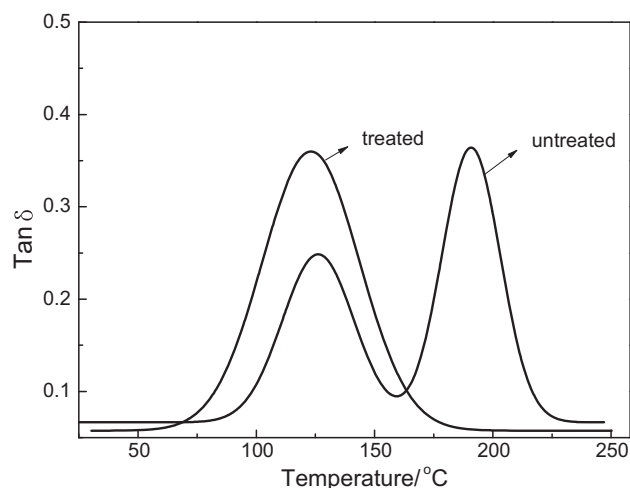


Fig. 4. The loss factors, $\tan \delta$, over temperature curves of the untreated and treated samples after aging 90 days at $150\text{ }^\circ\text{C}$.

which are controlled by oxygen diffusion are different at the interior and exterior. Hence the third possibility is proved to be correct.

The results of ATR-FTIR can show the changes of chemical structure at the surface of the samples. According to the ATR-FTIR analyses, the chain scission may occur in many positions in the network, leading to the scission of bridge between benzene rings in DGEBA and dangling chains in EPN, and then they escape from the system in the form of small molecules. Molecular rearrangements may occur among the remainders, resulting in the formation of more stable compound, with a higher concentration of benzene ring and crosslink density, so it has a higher glass transition temperature.

Fig. 5 shows glass transition temperature and the $\tan \delta$ peak value over aging time. T_{g1} and $\tan \delta_1$ are the glass transition temperature and $\tan \delta$ peak intensity of the interior compound, and T_{g2} and $\tan \delta_2$ are related to the new compound. In the initial period of aging, T_{g1} rises with the increasing of aging time, and $\tan \delta_1$ decreases, which are attributed to the post-cure process [31,32]. After 15 days' aging, T_{g1} begins to decrease because of the oxidative degradation of the interior compound. However, $\tan \delta_1$ does not rise accordingly; instead, it declines with the increase of aging time, because of the increase thickness of the oxide layer. T_{g2} increases firstly and then tends to be a constant value; $\tan \delta_2$ keeps rising in all aging time range. This might be due to the degree of oxidation and degradation and the increase thickness of the oxide layer.

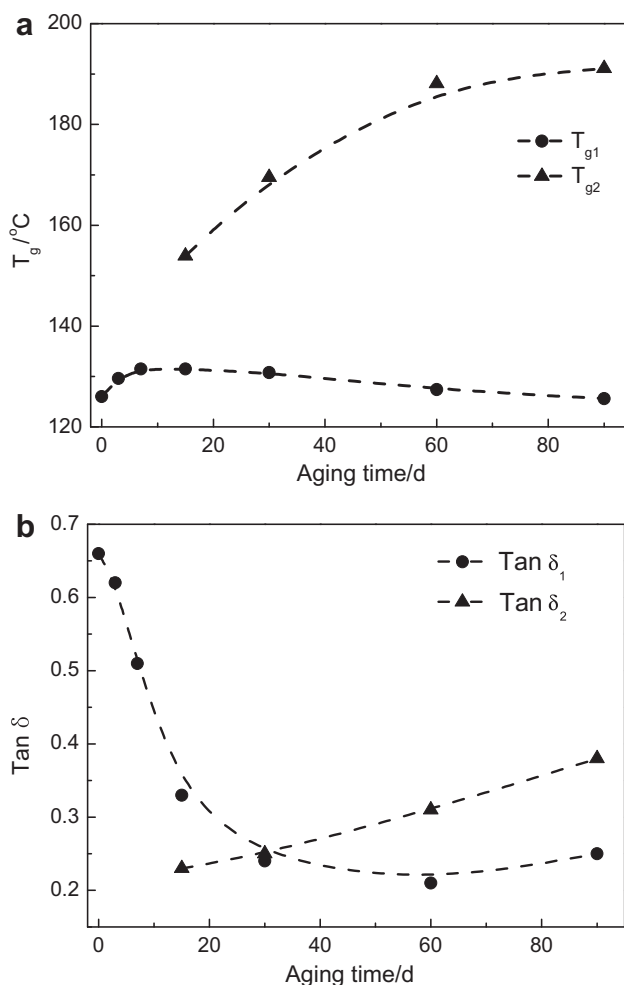


Fig. 5. Glass transition temperature and the $\tan \delta$ peak value over aging time curves at $150\text{ }^\circ\text{C}$ (T_{g1} and $\tan \delta_1$ are for matrix, and T_{g2} and $\tan \delta_2$ are related to the new phase).

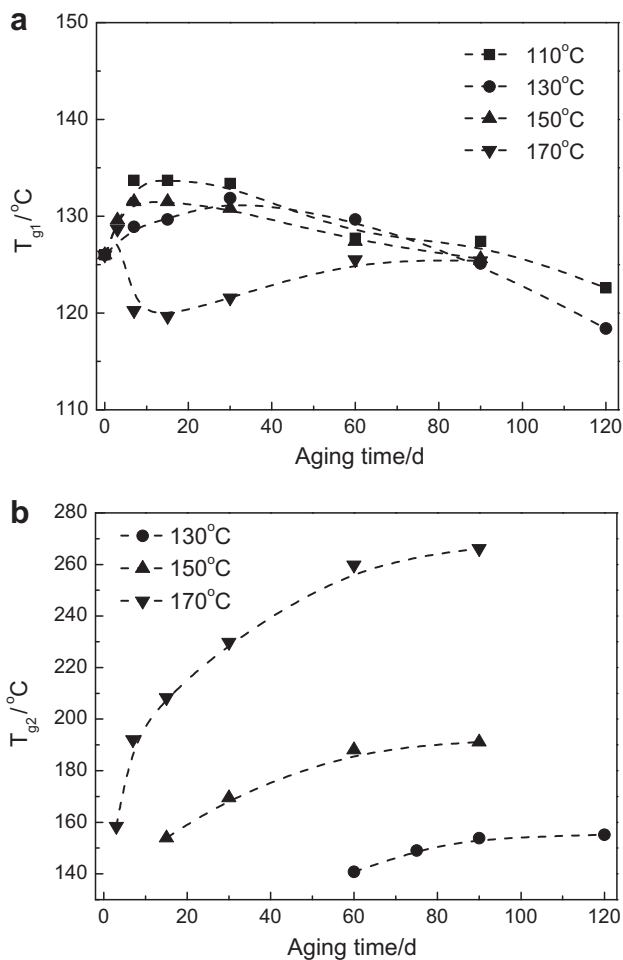


Fig. 6. Curves of glass transition temperature T_g over aging time at different temperature (T_{g1} represents T_g of matrix phase, T_{g2} represents T_g of new phase).

3.3. Influence of temperature on thermal–mechanical properties

The changes of glass transition temperature T_g during thermal-oxidative aging of samples are shown in Fig. 6. The glass transition temperature of the internal compound (T_{g1}) increases in the initial period when post-cure predominates and decreases when chain

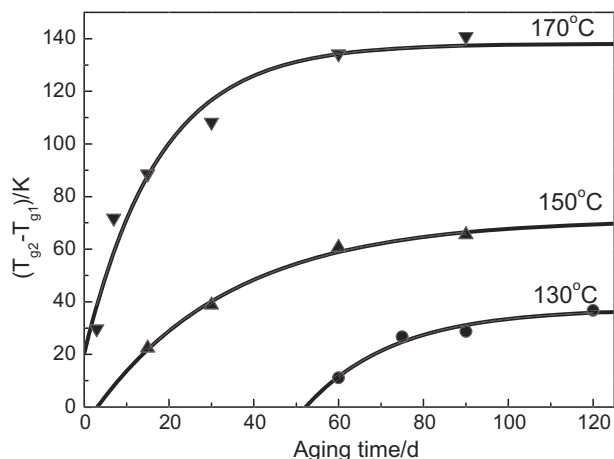


Fig. 7. Nonlinear regression curves of $(T_{g2} - T_{g1})$ over aging time.

Table 2 Results of nonlinear regression.

T_a/K	A/K	k/d^{-1}	$\Delta T_{g\infty}/K$
403	-451.6	0.048	37.3
423	-78.4	0.031	71.4
453	-117.8	0.057	138.1

scission predominates. T_{g1} of the sample begins to rise again after aging at 170 °C for 15 days, which can be attributed to the dehydration or other molecular rearrangements in the interior of the samples. New glass transition temperature T_{g2} appears at 3d, 15d and 60d, aged at 170 °C, 150 °C and 130 °C respectively. When the samples have been aged at 110 °C for 120 days, glass transition of a new more stable compound at the surface is not observed by DMTA. The material is in the glassy state at 110 °C, so chain scissions and molecular rearrangements are hard to occur. Therefore, T_{g1} only has a little reducing due to the chain scission after 120 days' aging at 110 °C. In addition, T_{g2} is increasing exponentially dependent on the aging time as shown in Fig. 5b.

T_{g2} is glass transition temperature of new formed compound at the surface of the samples, and T_{g1} is glass transition temperature of the internal compound. The difference between them can reflect the difference of oxidative degradation degree between surface and interior of the samples for the different oxygen concentration. Therefore, the difference (ΔT_g) as function of aging time is shown in Fig. 7. Fig. 7 also shows the results of nonlinear regression based on formula (2) shown as follows:

$$\Delta T_g = A \exp(-kt_a) + \Delta T_{g\infty} \quad (2)$$

where A and k are constants related to aging temperature, $\Delta T_{g\infty}$ is value of $(T_{g2} - T_{g1})$ when aging time (t_a) tends to infinity ($t_a \rightarrow \infty$).

The results of nonlinear regression are shown in Table 2. Both k and A do not vary regularly with aging temperature (T_a). This is possible since they are influenced by concentration of oxygen besides aging temperature. However, it is known that linear relative coefficient of $\ln(T_{g2} - T_{g1})_{\infty}$ and $1/T_a$ is 0.9978 through linear fitting. The result of linear fitting is shown in Fig. 8, and an experience formula between $\Delta T_{g\infty}$ and T_a is obtained as formula (3),

$$\Delta T_{g\infty} = 6.97 \times 10^6 \exp(-5825/T_a) \quad (3)$$

where $\Delta T_{g\infty}$ is the difference between T_{g2} and T_{g1} after being aged for indefinite time, and T_a is the aging temperature.

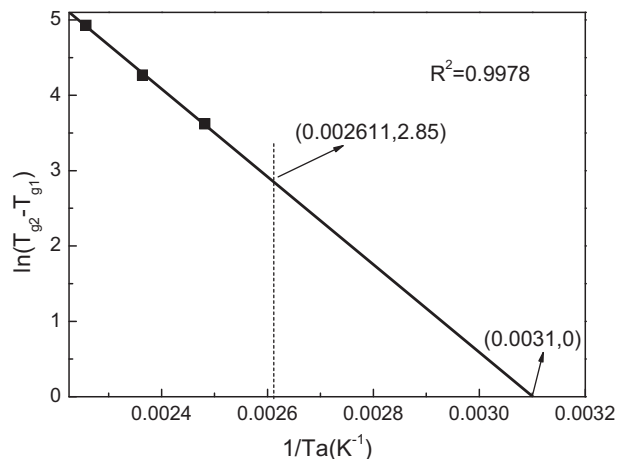


Fig. 8. Result of linear fitting with $\ln(T_{g2} - T_{g1}) \sim 1/T_a$.

$\Delta T_{g\infty}$ at different aging temperature (T_a) can be obtained through formula (3). When T_a is 110 °C, $\Delta T_{g\infty}$ is 16.1 °C, which means that it is possible for the system to form a new compound after aging enough time at 110 °C. When T_a is room temperature 25 °C, $\Delta T_{g\infty}$ is 0.022 °C. It is suggested that serious oxidative degradation which lead to the increase glass transition temperature hardly occurs at room temperature.

4. Conclusions

The article deals with the thermal-oxidative aging of diglycidyl ether of bisphenol-A and novolac epoxy resin blends cured with low molecular polyamide (DGEBA/EPN/LMPA system). The results of ATR-FTIR and DMTA measurements lead to the following conclusions:

- (1) Post-cure reactions occur in the initial period of aging. Besides, methylenes in many positions are oxidized to carbonyl and C–C, C–N and C–O bonds break in the later stage of thermal-oxidative aging.
- (2) At the surface of the sample, the bridges between benzene rings in DGEBA and dangling chains in EPN are broken, and escape from the system as small molecules. Dehydration or other molecular rearrangement occurs among the remainders.
- (3) The degree of oxidation and degradation controlled by oxygen diffusion are different in the interior and exterior of the sample, which lead to the formation of “skin-core” structure. For the interior compound, the glass transition temperature rises for post-cure at first, then decline for scission degradation. For the exterior compound, the glass transition temperature with aging time follows an exponential law.
- (4) When the samples are aging at 170 °C, 150 °C and 130 °C, a new glass transition appears at about 3d, 15d and 60d, respectively. And there is linear correlation between $\ln(T_{g2}-T_{g1})_{\infty}$ and $1/T_a$.

References

- [1] Damian C, Espuche E, Escoubes M. Influence of three ageing types (thermal oxidation, radiochemical and hydrolytic ageing) on the structure and gas transport properties of epoxy-amine networks. *Polym Degrad Stab* 2001; 72(3):447–58.
- [2] Devanne T, Bry A, Audouin L, Verdu J. Radiochemical ageing of an amine cured epoxy network. Part I: change of physical properties. *Polymer* 2005;46(1): 229–36.
- [3] Buch X, Shanahan MER. Influence of the gaseous environment on the thermal degradation of a structural epoxy adhesive. *J Appl Polym Sci* 2000;76(7): 987–92.
- [4] Hodge IM. Physical aging in polymer glasses. *Science* 1995;267:1945–7.
- [5] Maddox SL, Gillham JK. Isothermal physical aging of a fully cured epoxy-amine thermosetting system. *J Appl Polym Sci* 1997;64:55–67.
- [6] Barral L, Cano J, Lopez J, Lopez-Bueno I, Nogueira P, Abad MJ, et al. Physical aging of a tetrafunctional/phenol novolac epoxy mixture cured with diamine: DSC and DMA measurements. *J Therm Anal Calorim* 2000;60(2):391–9.
- [7] Cherdoud-Chihani A, Mouzali M, Abadie MJM. Study of crosslinking AMS/DGEBA system by FTIR. *J Appl Polym Sci* 1998;69:1167–78.
- [8] Bockenheimer C, Fata D, Possart W. New aspects of aging in epoxy networks I. Thermal aging. *J Appl Polym Sci* 2004;9:361–8.
- [9] Barral L, Cano J, Lopez AJ, Lopez J, Nogueira P, Ramirez C. Thermal degradation of a diglycidyl ether of bisphenol A/1, 3-bisaminomethyl-cyclohexane (DGEBA/1, 3-BAC) epoxy resin system. *Thermochim Acta* 1995;269/270: 253–9.
- [10] Mailhot B, Morlat-Therias S, Ouahioune M, Gardette JL. Study of the degradation of an epoxy/amine resin. *Macromol Chem Phys* 2005;206:575–84.
- [11] Hong SG. The thermal-oxidative degradation of an epoxy adhesive on metal substrates: XPS and RAIIR analyses. *Polym Degrad Stab* 1995;48(2):211–8.
- [12] Dao B, Hodgkin J, Krstina J, Mardel J, Tian W. Accelerated aging versus realistic aging in aerospace composite materials. II. Chemistry of thermal aging in a structural composite. *J Appl Polym Sci* 2006;102:3221–32.
- [13] Musto P, Ragosta G, Russo P, Mascia L. Thermal-oxidative degradation of epoxy and epoxy-bismaleimide networks: kinetics and mechanism. *Macromol Chem Phys* 2001;202:3445–58.
- [14] Galant C, Fayolle B, Kuntz M, Verdu J. Thermal and radio-oxidation of epoxy coatings. *Progr Org Coating* 2010;69(4):322–9.
- [15] Decelle J, Huet N, Bellenger V. Oxidation induced shrinkage for thermally aged epoxy networks. *Polym Degrad Stab* 2003;81(2):239–48.
- [16] Buch X, Shanahan MER. Thermal and thermo-oxidative ageing of an epoxy adhesive. *Polym Degrad Stab* 2000;68(3):403–11.
- [17] Chen JS. Controlled degradation of epoxy networks: analysis of crosslink density and glass transition temperature changes in thermally reworkable thermosets. *Polymer* 2004;45:1939–50.
- [18] Budrugaec P, Segal E. Application of isoconversional and multivariate non-linear regression methods for evaluation of the degradation mechanism and kinetic parameters of an epoxy resin. *Polym Degrad Stab* 2008;93(6): 1073–80.
- [19] Montserrat S. Physical aging studies in epoxy resins. I. Kinetics of the enthalpy relaxation process in a fully cured epoxy resin. *J Polym Sci B Polym Phys* 1994; 32:509–22.
- [20] Xian G, Karbhari VM. DMTA based investigation of hygrothermal ageing of an epoxy system used in rehabilitation. *J Appl Polym Sci* 2007;104:1084–94.
- [21] Devanne T, Bry A, Audouin L, Verdu J. Radiochemical ageing of an amine cured epoxy network. Part II: kinetic modelling. *Polymer* 2005;46(1):237–42.
- [22] Delor-Jestin F, Drouin D, Cheval PY, Lacoste J. Thermal and photochemical aging of epoxy resin-Influence of curing agents. *Polym Degrad Stab* 2006; 91(6):1247–55.
- [23] Awaja F, Pigram PJ. Surface molecular characterisation of different epoxy resin composites subjected to UV accelerated degradation using XPS and ToF-SIMS. *Polym Degrad Stab* 2009;94(4):651–8.
- [24] Shukla V, Shukla R, Singh D, Singh M, Bajpai M, Seth S. Development of polyamide curable modified epoxy novolac resins with improved adhesion and chemical resistance. *Pigm Resin Technol* 2005;34(2):66–71.
- [25] Unnikrishnan KP, Thachil ET. Effect of phenol/formaldehyde stoichiometry on the modification of epoxy resin using epoxidized novolacs. *Int J Polym Mater* 2006;55:385–98.
- [26] Unnikrishnan KP, Thachil ET. Aging and thermal studies on epoxy resin modified by epoxidized novolacs. *Polym Plast Technol Eng* 2006;45:469–74.
- [27] Mathew D, Reghunadhan NCP, Ninan KN. Bisphenol A dicyanate-novolac epoxy blend: cure characteristics, physical and mechanical properties, and application in composites. *J Appl Polym Sci* 1999;74:1675–85.
- [28] Monney L, Belali R, Vebrél J, Dubois C, Chambaudet A. Photochemical degradation study of an epoxy material by IR-ATR spectroscopy. *Polym Degrad Stab* 1998;62:353.
- [29] Rivaton A, Moreau L, Gardette JL. Photo-oxidation of phenoxy resins at long and short wavelengths-I. Identification of the photoproducts. *Polym Degrad Stab* 1997;58:321.
- [30] Audouin L, Langlois V, Verdu J, Bruijn JCM. Role of oxygen diffusion in polymer ageing: kinetic and mechanical aspects. *J Mater Sci* 1994;29(3):569–83.
- [31] Pang KP, Gillham JK. Competition between cure and thermal degradation in a high T_g epoxy system: effect of time and temperature of isothermal cure on the glass transition temperature. *J Appl Polym Sci* 1990;39:909–33.
- [32] Dyakonov T, Chen Y, Holland K. Thermal analysis of some aromatic amine cured model epoxy resin systems – I: materials synthesis and characterization, cure and post-cure. *Polym Degrad Stab* 1996;53(2):217–42.